Baltic Astronomy, vol. 00, 000–000, 2016

ESTIMATION OF THE VERTICAL DISK SCALE HEIGHT USING YOUNG GALACTIC OBJECTS

V.V. Bobylev and A.T. Bajkova

Central (Pulkovo) Astronomical Observatory of RAS, 65/1 Pulkovskoye Ch., St. Petersburg, Russia; bob-v-vzz@rambler.ru

Abstract. We have collected literature data on young Galactic objects such as masers with VLBI-measured trigonometric parallaxes, OB associations, HII regions and Cepheids. We have recently established that vertical disk scale height is strongly influenced by the objects of the Local arm. In the present work we used samples that do not contain objects in this arm. Based on the model of a self-gravitating isothermal disk for the density distribution, we have found the following vertical disk scale heights: $h = 46 \pm 5$ pc from 69 masers with trigonometric parallaxes, $h = 36 \pm 3$ pc from 59 OB associations, $h = 35.6 \pm 2.7$ pc from 147 HII regions, $h = 52.1 \pm 1.9$ pc from 195 young Cepheids, and $h = 72.0 \pm 2.3$ pc from 192 old Cepheids.

Key words: ISM: structure – Galaxy (Milky Way): kinematics and dynamics

arXiv:1609.01129v2 [astro-ph.GA] 6 Sep 2016

1. INTRODUCTION

The Galactic thin disk attracts the attention of many authors. Data on young O- and B-type stars, open clusters, Cepheids, infrared sources, molecular clouds, and other young objects are used to study its properties. In particular, such parameters as the offset of the symmetry plane relative to the Sun $z_\odot$ and the vertical disk scale height h are important.

Previously (Bobylev & Bajkova 2016a), we showed the z distribution of Galactic masers with measured trigonometric parallaxes to be asymmetric. We suggested that this is because the sample is dominated by the masers observed mainly from the Earth's northern hemisphere. However, there can also be other sources of this peculiarity, which should be studied using a large statistical material. In particular, it is interesting to check the influence of the Local arm. As we showed previously (Bobylev & Bajkova 2014), the symmetry plane of the Local arm has an inclination of about 6° to the Galactic plane. Since about 40 of the 130 masers belong to the Local arm, the effect here can be significant.

In paper of Bobylev & Bajkova (2016b) the approach, based on exclusion of the objects of the Local arm, was applied for analysis of samples of Galactic objects for which the distances were determined using the kinematic method. In the present work we are going to apply this approach for the analysis of samples, the distances to which are determined with higher precision, from 10% (trigonometric parallaxes) to 15%–25% ("period-luminosity" or spectrophotometric distances).

2. METHOD

We use heliocentric rectangular coordinate systems xyz where the x axis is directed toward the Galactic center, the y axis is in the direction of Galactic rotation,

and the z axis is directed to the north Galactic pole.

In the case of an exponential density distribution, the observed distribution of objects along the z coordinate axis is described by the expression

$$N(z) = N_1 \exp\left(-\frac{|z - z_\odot|}{h_1}\right). \quad (1)$$

If the model of a self-gravitating isothermal disk is used for the density distribution, then the observed distribution of objects along the z axis is described by

$$N(z) = N_2 \ \mathrm{sech}^2\left(\frac{z - z_\odot}{\sqrt{2}\ h_2}\right). \quad (2)$$

Finally, the observed distribution of objects along the z axis for the Gaussian model is described by the formula

$$N(z) = N_3 \exp\left[-\frac{1}{2}\left(\frac{z - z_\odot}{h_3}\right)^2\right]. \quad (3)$$

In (1)–(3) N_i, $i = 1, 2, 3$, are the normalization coefficients, $z_\odot$ is the offset of the symmetry plane relative to the Sun, and h_i are vertical disk scale parameters (in case of $i = 1$ is so called "scale height").

3. DATA

(1) We use the data on known OB associations with reliable distance estimates from Mel'nik & Dambis (2009). The distances derived by these authors were reconciled with the Cepheid scale. The catalog contains 91 OB associations; the distances to them do not exceed 3.5 kpc.

(2) We use a sample of Galactic masers with measured trigonometric parallaxes. These sources, associated with very young stars, are located in regions of active star formation. Highly accurate astrometric VLBI measurements of the trigonometric parallaxes and proper motions have already been performed for more than 130 such masers by several teams in the USA, Japan, Europe, and Australia (Reid et al. 2014; Bobylev et al. 2016; Rastorguev et al. 2016). The error in the stellar parallax determined by this method is, on average, less than 10%. For these objects we use the following restriction on heliocentric distance $r < 6$ kpc. For all objects we use the restriction on r in order to avoid the influence of bending of the disk (Bobylev 2013).

(3) We supplemented the well-known catalog of HII regions (Russeil 2003) with new photometric estimates of the distances to several star-forming regions collected in Russeil et al. (2007) and Moisés et al. (2011). From this catalog we took only those distances that were obtained photometrically. For these objects we use the restriction $r < 4.5$ kpc.

(4) We use the sample of classical Cepheids belonging to our Galaxy described by Mel'nik et al. (2015). This sample contains 674 stars whose distances were determined from the most recent calibrations using both optical and infrared photometric observational data. We have two samples of Cepheids with mean ages ≈ 75 and ≈ 138 Myr. For these objects we use the restriction $r < 4$ kpc.

Table 1: The offset of the symmetry plane relative to the Sun $z_\odot$ and the vertical disk scale height h_i, $i = 1, 2, 3$ obtained using models (1), (2) and (3) from samples with trigonometric, spectrophotometric or "period-luminosity" distances

$z_\odot$, pc	h_1, pc	h_2, pc	h_3, pc	Sample
-18 ± 5	51 ± 5	46 ± 5	54 ± 5	69 masers with parallaxes
-13 ± 4	46 ± 3	36 ± 3	45 ± 3	59 OB associations
-14 ± 4	46.6 ± 2.8	35.6 ± 2.7	48.4 ± 2.8	147 HII regions
-26 ± 2	64.1 ± 2.4	52.1 ± 1.9	68.2 ± 2.5	195 young Cepheids
-26 ± 2	83.1 ± 2.4	72.0 ± 2.3	85.2 ± 2.8	192 old Cepheids

According to Bobylev & Bajkova (2014), we took a 6.2×1.1 kpc rectangle oriented at an angle of $-13°$ to the y axis and displaced from the Sun by 0.3 kpc toward the Galactic anticenter as the simplest Local-arm model (see Fig. 1–2 in Bobylev & Bajkova 2016b). For a sample of masers with measured trigonometric parallaxes, we use the division into spiral arms according to Reid et al. (2014).

4. RESULTS AND DISCUSSION

In Table 1 the offset of the symmetry plane relative to the Sun $z_\odot$ and the vertical disk scale height h_i, $i = 1, 2, 3$ obtained using models (1)–(3) are given. These parameters and their errors were found by fitting the models to the histograms and through Monte-Carlo simulations. For this purpose, we constructed the histograms with a step of 20 pc in z coordinate. As can be seen from the Table 1 the values of h_1 and h_3 are close each other, so in the Figures we quote only two lines: for models (1) and (2).

The histogram in the left panel of Fig. 1, shown without fill, was built using the whole sample of 113 masers ($r < 6$ kpc). The histogram in the left panel of Fig. 1, shown with fill, was constructed using 44 masers of the Local arm. As clearly seen from this figure, the maximum value of the distribution of masers from the Local arm falls on the positive z. Moreover, it is noticeable the strong influence of the Local arm masers on the distribution of the whole sample, so we make a conclusion about the need to exclude objects of the Local arm. On the right panel of Fig. 1 it is presented a histogram constructed using 69 masers, without objects of the Local arm.

Histograms built on OB associations, HII regions, young and old Cepheids are given in Fig. 2. From the comparison with the results obtained on these samples, without exception Local arm objects (Bobylev & Bajkova 2016a), can see a significant improvement in the histograms (they become closer to the Gaussian) of masers and OB associations. Previously (Bobylev and Bajkova 2016a), we have found the following vertical disk scale heights: $h_2 = 40.2 \pm 2.1$ pc from 91 OB associations, $h_2 = 48.4 \pm 2.5$ pc from 187 HII regions, $h_2 = 60.1 \pm 1.9$ pc from 246 young Cepheids, and $h_2 = 72.5 \pm 2.3$ pc from 250 old Cepheids. We see that after the exception objects Local arm, the value of h is always decreasing.

Bobylev & Bajkova (2016b) have obtained the following estimates from objects located in the inner region of the Galaxy: $z_\odot = -5.7 \pm 0.5$ pc and $h_2 = 24.1 \pm 0.9$ pc from the sample of 639 methanol masers, $z_\odot = -7.6 \pm 0.4$ pc and $h_2 = 28.6 \pm 0.5$ pc from 878 HII regions, $z_\odot = -10.1 \pm 0.5$ pc and $h_2 = 28.2 \pm 0.6$ pc from 538 giant

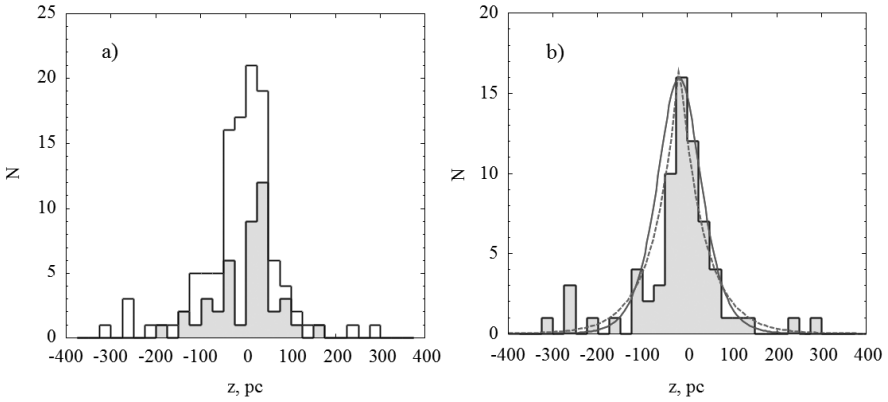

Fig. 1. Histograms of the z distribution of masers: the whole sample (without fill pattern), masers belonging to the Local arm (fill pattern) (a), the sample without masers belonging to the Local arm, the dashed and solid lines represent models (1) and (2), respectively (b).

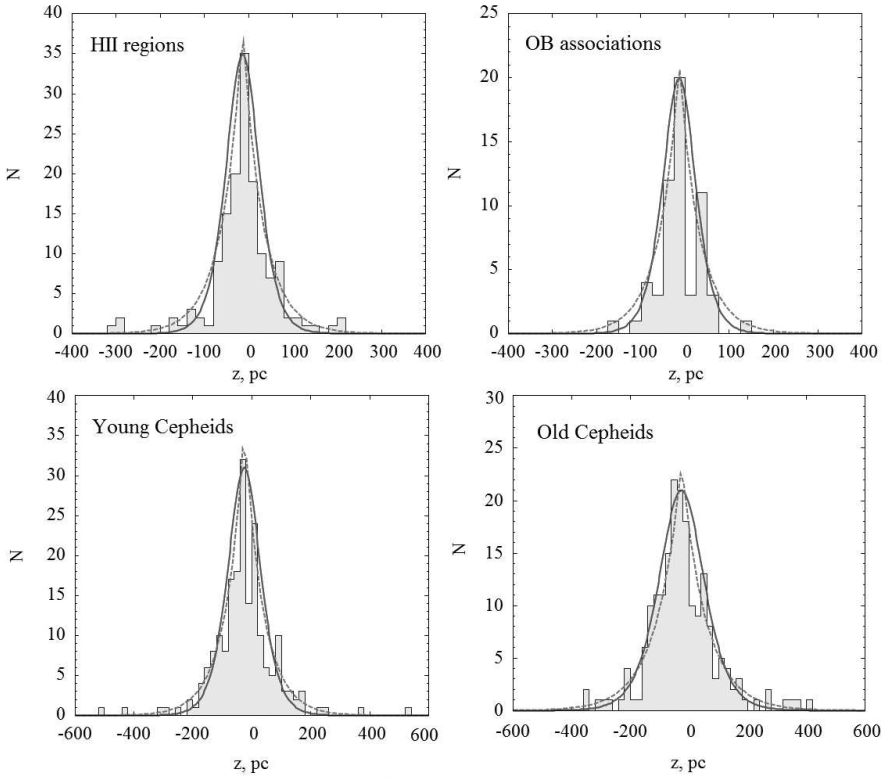

Fig. 2. Histograms of the z distributions of 59 OB associations, 147 HII regions, 195 young Cepheids and 192 old Cepheids. The dashed and solid lines on all panels represent models (1) and (2), respectively.

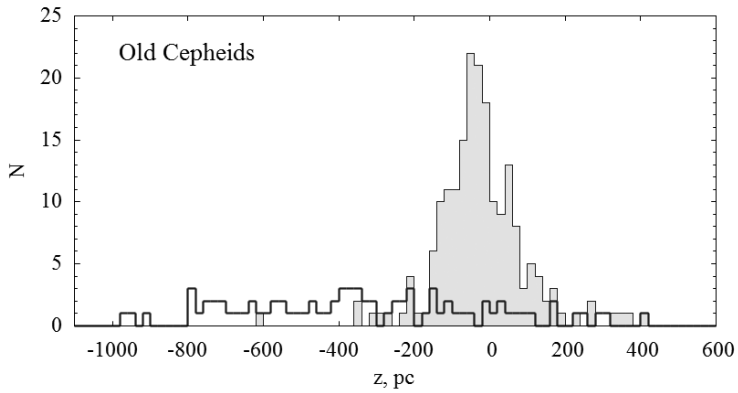

Fig. 3. Histograms of the z distribution of old Cepheids: the sample with heliocentric distance $4 < r < 10$ kpc (without fill pattern) and the sample with distances $r < 4$ kpc (fill pattern).

molecular clouds.

A detailed overview of the parameters $z_\odot$ and h, obtained by different authors, can be found in work of Bobylev & Bajkova (2016a). Here we only note the result of the analysis of the extensive sample of giant molecular clouds (the ATLASGAL program) with kinematic distances from the work of Wienen et al. (2015). These authors found $z_\odot \sim -7 \pm 1$ pc and $h \sim 28 \pm 2$ pc.

It is interesting to note that the broad wings on the histograms of z distributions are observed practically in each of our samples (see Fig. 1–2), with the exception of OB associations. The wings are also visible in the histogram of Wolf-Rayet stars (Fig. 2 in Bobylev & Bajkova 2016a) and methanol masers (Fig. 6 in Bobylev & Bajkova 2016b). Thus we see that (i) the histogram wings are always better approximated by model (1), (ii) all three models do not end up describing the wide wings.

A detailed study of all effects leading to the formation of wide wings on the histograms is the subject of a separate research due to the great complexity of the problem. Here we would like to mention only one of the possible causes associated with the warp of the galactic disk (Bobylev 2013). For this, we use the old Cepheids. In Fig. 3 there are two histograms built using two different samples. The first sample consists of 192 Cepheids, located at distances $r < 4$ kpc (also shown in Fig. 2) and the second sample includes 81 Cepheids of the distance interval $4 < r < 10$ kpc. As can be seen from Fig. 3, the distribution of distant Cepheids (second sample) is considerably shifted toward the negative z and has a much bigger variance compared to the distribution of the Cepheids of the first sample: it can be described, for example, on the basis of model (3) with the following parameters: $z_\odot = -321$ pc and $h_3 = 241$ pc. Thus, we have two distributions with very different properties. So the presence of broad wings on the histograms of z-distributions is possible due to the penetration of objects with properties of the second sample in the first sample due to large measurement errors of the distances of the objects.

5. CONCLUSIONS

To study the vertical distribution of visible matter in the thin disk of the Galaxy we used several samples of young objects from the solar neighbourhood of radius no more than 4.5 kpc (for masers no more than 6 kpc). In the sample of masers with measured parallaxes, it is shown that in this task, it is better not to use the objects of the Local arm.

To each of these samples, we applied three models of the density distribution: the model of an exponential distribution, the model of a self-gravitating isothermal disk, and the model of a Gaussian density distribution. The results obtained based on models (1) and (3) are very close.

Based on the model of an exponential distribution, we have found the following vertical disk scale heights: $h_1 = 51 \pm 5$ pc from 69 masers with trigonometric parallaxes, $h_1 = 46 \pm 3$ pc from 59 OB associations, $h_1 = 46.6 \pm 2.8$ pc from 147 HII regions, $h_1 = 64.1 \pm 2.4$ pc from 195 young Cepheids (Age$\approx$75 Myr), and $h_1 = 83.1 \pm 2.4$ pc from 192 old Cepheids (Age$\approx$138 Myr).

Based on the model of a self-gravitating isothermal disk, we have found the following vertical disk scale heights: $h_2 = 46 \pm 5$ pc from masers, $h_2 = 36 \pm 3$ pc from OB associations, $h_2 = 35.6 \pm 2.7$ pc from HII regions, $h_2 = 52.1 \pm 1.9$ pc from young Cepheids, and $h_2 = 72.0 \pm 2.3$ pc from old Cepheids.

ACKNOWLEDGMENTS. We are grateful to the referee for his helpful remarks that contributed to an improvement of this paper. This study was supported by the "Transient and explosive processes in astrophysics" Program of the Presidium of Russian Academy of Sciences (P–7).

REFERENCES

Bobylev V. V., 2013, Astron. Lett., 39, 753
Bobylev V. V., Bajkova A. T., 2014, Astron. Lett., 40, 783
Bobylev V. V., Bajkova A. T., 2016a, Astron. Lett., 42, 1
Bobylev V. V., Bajkova A. T., 2016b, Astron. Lett., 42, 182
Bobylev V. V., Bajkova A. T., and Shirokova K. S., 2016, Balt. Astron., 25, 15
Mel'nik A. M., Dambis A. K., 2009, MNRAS, 400, 518
Mel'nik A. M., Rautiainen P., Berdnikov L. N. et al., 2015, AN, 336, 70
Moisés A. P., Damineli A., Figueredo E. et al., 2011, MNRAS, 411, 705
Rastorguev A. S., Zabolotskikh M. V., Dambis A. K. et al., 2016, arXiv: 1603.09124
Reid M. J., Menten K. M., A. Brunthaler A. et al., 2014, ApJ, 783, 130
Russeil D., 2003, A&A, 397, 133
Russeil D., Adami C., and Georgelin Y. N., 2007, A&A, 470, 161
Wienen M., Wyrowski F., Menten K. M. et al., 2015, A&A, 579, 91